

## Original Article


**Cite this article:** Banaee N, Goodarzi K, and Hosseinzadeh E. (2023) Comparison of neutron contamination in small photon fields of secondary collimator jaws and circular cones. *Journal of Radiotherapy in Practice*. **22**(e107), 1–6. doi: [10.1017/S1460396923000328](https://doi.org/10.1017/S1460396923000328)

Received: 26 May 2023  
Revised: 11 August 2023  
Accepted: 21 August 2023

**Keywords:**  
Monte Carlo; neutron contamination;  
photoneutron; radiotherapy; small fields

**Corresponding author:**  
Dr Nooshin Banaee;  
Email: [nooshin\\_banaee@yahoo.com](mailto:nooshin_banaee@yahoo.com)

# Comparison of neutron contamination in small photon fields of secondary collimator jaws and circular cones

Nooshin Banaee<sup>1</sup> , Kiarash Goodarzi<sup>1</sup> and Elham Hosseinzadeh<sup>2</sup>

<sup>1</sup>Medical Radiation Research Center, Central Tehran Branch, Islamic Azad University, Tehran, Iran and <sup>2</sup>Department of Medical Physics, Faculty of Medicine, Jundishapur University of Medical Sciences, Ahvaz, Iran

## Abstract

**Introduction:** Advanced treatment modalities involve applying small fields which might be shaped by collimators or circular cones. In these techniques, high-energy photons produce unwanted neutrons. Therefore, it is necessary to know neutron parameters in these techniques. **Materials and methods:** Different parts of Varian linac were simulated by MCNPX, and different neutron parameters were calculated. The results were then compared to photoneutron production in the same nominal fields created by circular cones. **Results:** Maximum neutron fluence for  $1 \times 1$ ,  $2 \times 2$ ,  $3 \times 3$  cm<sup>2</sup> field sizes was 165, 40.4, 19.78 (cm<sup>-2</sup>.Gy<sup>-1</sup> × 10<sup>6</sup>), respectively. The maximum values of neutron equivalent doses were 17.1, 4.65, 2.44 (mSv/Gy of photon dose) for  $1 \times 1$ ,  $2 \times 2$ ,  $3 \times 3$  cm<sup>2</sup> field size, respectively, and maximum neutron absorbed doses reached 903, 253, 131 (μGy/Gy photon dose) for  $1 \times 1$ ,  $2 \times 2$ ,  $3 \times 3$  cm<sup>2</sup> field sizes, respectively. **Conclusion:** Comparing the results with those in the presence of circular cones showed that circular cones reduce photoneutron production for the same nominal field sizes.

## Introduction

External beam radiotherapy (EBRT) is the most common and useful modality of cancer treatment. Linear accelerators (linacs) generate megavoltage electron and photon beams with different energies. High-energy photon and electron beams produce unwanted neutrons and deliver undesirable dose to patients. However, this extra dose is low but due to the high radiation quality factor of neutrons ( $w_R$ ), these particles have significant biological effects.<sup>1–3</sup> The rate of this phenomenon depends on energy of the incident photons and atomic number of the target. Therefore, radiotherapy with photon energies above 8 MeV usually consists of photonuclear process known as ( $\gamma$ , n) reaction which is the main source of neutron production. The NCRP 116 suggests a radiation quality factor of 20 for neutrons with energy of 0.1–2 MeV which might be produced in radiation therapy with photon beams. Considering the radiation quality factor of 20 for these photoneutrons shows the significant contribution of these particles in patients' effective doses and consequently in radiation-induced fatal cancer risks. Therefore, it is necessary to be aware of neutron portion in different treatment methods.<sup>4</sup>

To ensure delivering minimum dose to healthy structures, applying relatively small fields ( $0.3 \times 0.3$  cm<sup>2</sup>–  $4 \times 4$  cm<sup>2</sup>) is needed. For this purpose, there have been many developments in treatment machines. Small fields in EBRT are shaped by collimating a flattened or un-flattened high-energy photon beam using jaws, multi-leaf collimators (MLCs), circular cones, or adjustable tertiary collimators.<sup>5,6</sup>

Lately, Hosseinzadeh et al studied neutron contamination in the presence of circular cones.<sup>7</sup> However, there is no quantified comparison of neutron contamination due to circular cones and secondary collimator jaws which are both required in delivering different treatment techniques.

Since neutron dose measurements are accompanied by intensive gamma irradiation which cause uncertainty in photon fields, the dead time and pileup affects will falsify the results of experimental measurements.<sup>8</sup> The dosimetry of mixed photon-neutron fields represents frequent problems concerning the measurement/discrimination of dose contribution of different radiation components due to the complexity of neutron interactions with tissue, dosimeter, and ambient materials together with a wide range of the neutron energy. To overcome the difficulties of the measurements, numerical simulations with Monte Carlo (MC) codes would allow a detailed analysis of each component of mixed fields with the aim to compensate for the lack of the precision in measurements.<sup>9–12</sup>

The aim of this study is to calculate different neutron contamination parameters such as neutron fluence, neutron absorbed dose, and neutron equivalent dose in small 18 MV photon fields by MC MCNPX simulation and compare those created in presence of circular cones.

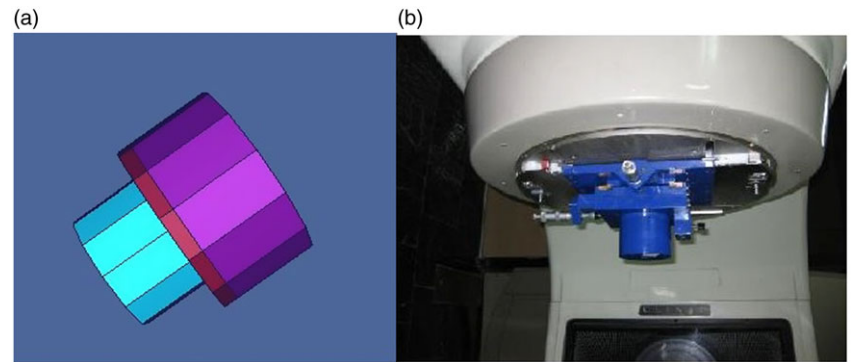


**Figure 1.** Circular cone: a. Schematic view of a circular cone, b. circular cone attachment to the gantry.

## Materials and Methods

At the onset of the study, MCNPX 2.6 was used to simulate the Varian Clinac 2100 C/D linac producing 18 MV photon beams. In order to provide a precise information of this machine, detailed geometry and materials data consist of target (W, Cu), primary collimator (W), flatterer filter (Ta, Fe), ion chambers (Kapton), and collimators (W) were simulated according to the information provided by the manufacturer. Moreover, a  $50 \times 50 \times 50 \text{ cm}^3$  water phantom with the source surface distance (SSD) of 100 cm was simulated, as well. The most important part of MC calculation is the validation of the simulation. Therefore, percentage depth dose (PDD) and beam profile at depth of 5 cm in water phantom were calculated for a  $10 \times 10 \text{ cm}^2$  field size. For PDD calculation, small cylindrical cells with the radius of 1 cm and thickness of 2 mm at the central axis were simulated. Calculation of beam profile was also performed in  $0.2 \text{ cm} \times 1.5 \text{ cm} \times 1 \text{ cm}$  cells which were located at the vertical direction of the central axis at depth of 5 cm in the water phantom. For both parameters, the energy deposited in each scoring cell was calculated by \*F8 tally and then was divided to the maximum value. Source definition of this simulation was defined to produce electron—photon beams with the maximum energy of 18.35 MeV and the Gaussian energy distribution with a full width at half maximum (FWHM) of 1 MeV. For validation purpose, code was run with  $2 \times 10^9$  histories which resulted in the statistical uncertainty of about 3%. Then, the results of this calculation were compared with those of practical measurements obtained by a Semiflex ionisation chamber (PTW, Freiburg, Germany).

In order to activate photoneutron generation in the MC simulation process, the fourth entry of Phys:p card was changed to -1; thus, neutrons which are produced by  $(\gamma, n)$  reactions would be tracked. Three different field sizes shaped by secondary collimators,  $1 \times 1$ ,  $2 \times 2$ , and  $3 \times 3 \text{ cm}^2$ , were simulated to calculate different parameters of neutrons, and the code was run with  $2 \times 10^9$  histories in electron-photon-neutron mode.

Neutron fluence in terms of (number  $\text{cm}^2$  /electron) and neutron absorbed dose in terms of ((MeV/g)/electron) were calculated by F4 tally and F6 tally, respectively. Additionally, the dose conversion capability provides several standard default dose functions. Therefore, dose function (DF) card was used to calculate the neutron equivalent dose in terms of (mSv/ electron).

Since uncertainties of neutron calculations in photon treatment fields are more than acceptable ranges, therefore time computation reduction methods such as applying electron and photon cut-off energy (1 MeV), FCL (Forced-Collision) card to control the forcing of neutron or photon collisions in each cell and force these particles to interact with head of linac and EXT (Exponential Transform)

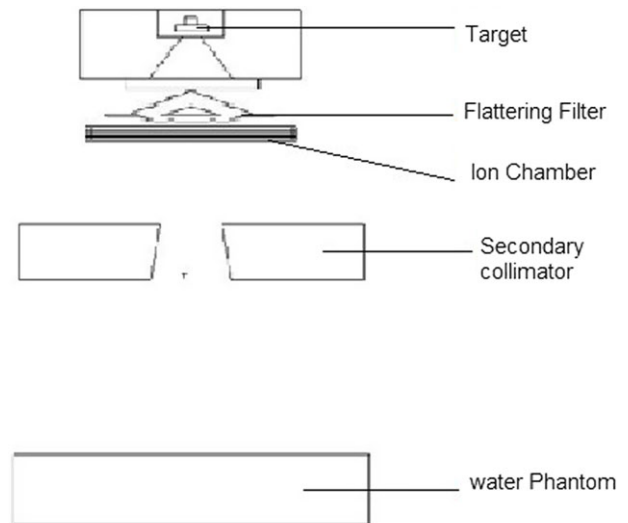


**Figure 2.** Simulated 18 MV Varian Clinac 2100 C/D linac

card to stretch the path length between collisions in a preferred direction and increase the weight of the neutrons in each cell were used. These cards increase accuracy of neutron calculation and decrease the statistical errors of the calculations to 2–3%.<sup>13</sup>

The other way to produce small photon fields in linac is using the circular cones made of lead that can be attached to a linac head as an accessory. Figure 1 shows a schematic view of a circular cone and how it can be attached to the linac. It is interesting to compare photoneutron production in small photon fields created by secondary collimators and circular cones. Therefore, neutron parameters of the fields created by secondary collimators were compared with those of circular cones reported in Hosseinzadeh et al. study.<sup>7</sup> The comparison was done between same nominal field sizes ( $1 \times 1$ ,  $2 \times 2$ ,  $3 \times 3 \text{ cm}^2$  square fields versus 1, 2, 3 cm circular ones).

## Results

Different parts of simulated Varian Clinac 2100 C/D linac producing 18 MV photon beams are depicted in Figure 2.

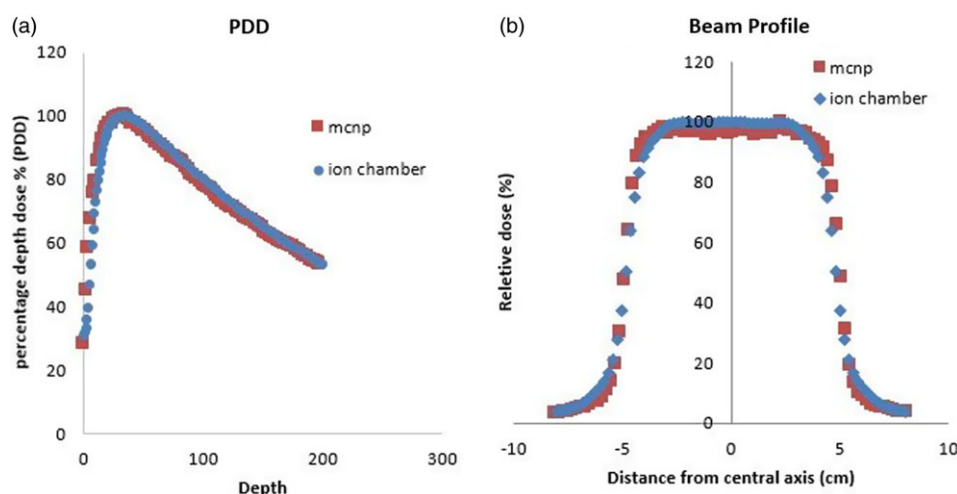
PDD and beam profile obtained by Semiflex ion chamber and MCNPX calculations for  $10 \times 10 \text{ cm}^2$  field size are shown in Figure 3. Additionally, Table 1 reports the results of validation and error calculation of this comparison.

**Table 1.** Simulation validation parameters: ion chamber measurements versus MC simulation

Beam profile	Parameters	Ion chamber	MC	Differences
	Max differences in flatness region	–	–	1.64%
	Max differences in the penumbra region	–	–	9.1%
	FWHM	9.6%	9.8%	0.2%
Percentage depth dose	Maximum difference at build-up region	–	–	0.58%
	$R_{50}$	0.56 cm	0.54 cm	0.02 cm
	$R_{80}$	1.2 cm	1.18 cm	0.02 cm
	$R_{90}$	1.62 cm	1.56 cm	0.06 cm
	Maximum dose point (cm)	3.4 cm	3.38 cm	0.02 cm

**Table 2.** Photon absorbed dose at ( $d_{max}$ ) for small field sizes shaped by secondary collimator jaws and circular cones<sup>7</sup>

Field size		Photon dose at $d_{max}$ (Gy/electron)	
Secondary collimator jaw (cm <sup>2</sup> )	Circular cone diameter (cm)	Secondary collimator jaws	Circular cones
1 × 1	1	3.54E-17	3.00E-16
2 × 2	2	1.45E-16	5.19E-16
3 × 3	3	3.26E-16	8.47E-16

**Figure 3.** Comparison of Semiflex ion chamber measurements and MC calculations for 10x10 cm<sup>2</sup>. a: PDD curve, b: beam profile

All results of MCNP are calculated per source initial particles (number of electrons prior to the target as number of histories). Thus, analysing these results in radiotherapy situation, normalisation of photoneutron production per Gy of delivered photon absorbed dose at each field size was required. Therefore, number of neutron, neutron equivalent dose, and neutron absorbed dose were normalised to the 1 Gy of photon dose in the maximum depth dose ( $d_{max}$ ).<sup>14,15</sup> With such method of calculation, the results of this study are comparable to the treatment situation. Table 2 shows the maximum photon dose at ( $d_{max}$ ) for small field sizes shaped by secondary collimator jaws and circular cones.

Figure 4 shows the neutron fluence per Gy of photon dose along the central axis for different field sizes shaped by jaws and circular cones. The number of neutrons per Gy of photon dose in secondary collimator for small fields is more than those of circular field. There are two reasons that number of neutrons per Gy of photon is less for circular cones:

- Circular cones and secondary collimators are made of lead and tungsten, respectively. Therefore, photons are more attenuated by lead (circular cone) compared to tungsten (secondary collimator). Attenuated photons produce less number of neutrons per Gy of photon. Therefore, neutrons per Gy of photon dose in secondary collimator for small fields are more than those of circular field.
- The comparison of number of neutrons per Gy of photon is done for nominally same field sizes (e.g., 1 cm<sup>2</sup> cone versus 1x1 cm<sup>2</sup> collimator). However, the area of these field sizes is not same and secondary collimator creates bigger field size compared to corresponding cone field. And as the field size increases, number of neutron per Gy of photon decreases which is consistent with previous publications.<sup>7</sup>

Table 3 indicates neutron fluence for small field sizes shaped by secondary collimator jaws and circular cones. As it is shown,

**Table 3.** Number of neutrons per Gy of photon dose for different field sizes<sup>7</sup>

Field size		Maximum calculated fluence (cm <sup>2</sup> Gy 1 × 10 <sup>6</sup> )		Maximum depth of fluence (cm)
Secondary collimator (cm <sup>2</sup> )	Circular cone diameter (cm)	Secondary collimator jaws	circular cones	
1 × 1	1	165	7.76	2
2 × 2	2	40.4	6.02	2
3 × 3	3	19.78	5.08	2

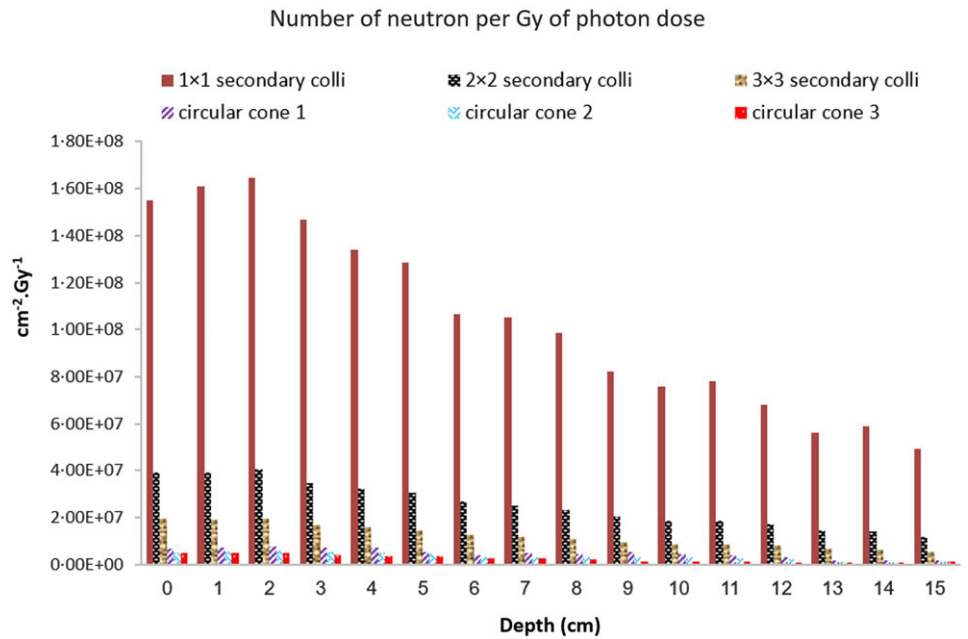


**Figure 4.** Number of neutrons per Gy of photon dose for different field sizes along the central axis

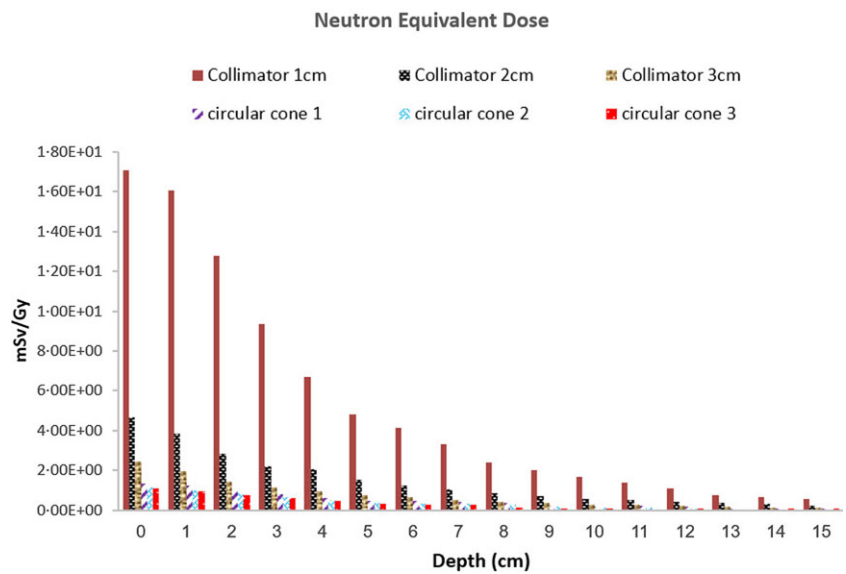


**Figure 5.** Comparison of neutron equivalent doses for various field sizes along the central axis

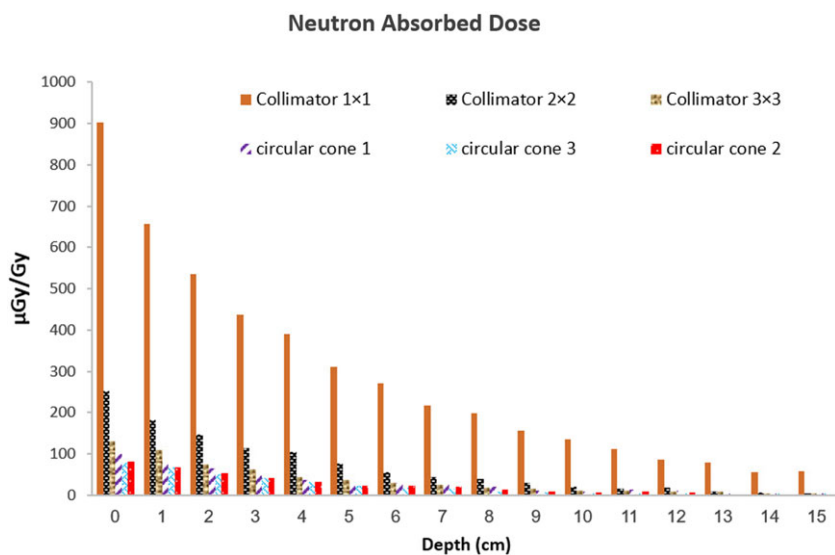
neutron fluence increased to a specific depth of phantom and then decreased monotonically by increasing depth. The largest value of neutron fluence appeared at depth of 2 cm in all field sizes, and as the field size decreases, neutron fluence increases. According to the neutron fluence in Figure 4, number of neutron per Gy of photon

dose in secondary collimator small fields is more than those of circular cones.

Figure 5 indicates the neutron equivalent dose along the central axis for different field sizes shaped by collimator jaws and circular cones. Table 4 shows the comparison of neutron equivalent doses

**Table 4.** Neutron equivalent dose for different field sizes<sup>7</sup>

Field size		Neutron equivalent dose (mSv/Gy)	
Secondary collimator (cm <sup>2</sup> )	Circular cone diameter (cm)	Secondary collimator jaws	circular cones <sup>12</sup>
1 × 1	1	17.1	1.31
2 × 2	2	4.65	1.12
3 × 3	3	2.44	1.08

**Figure 6.** Neutron absorbed dose along the central axis for different field sizes

for various field sizes. These results show that neutron equivalent dose has been decreased by increasing depth of phantom, and also the smallest field size has the largest value of neutron equivalent dose. Additionally, neutron equivalent dose in secondary collimator is more than circular cone fields. It shows that the cross-section of photoneutron interaction with high Z materials of cone and secondary collimator increases at smaller fields. Although the intensity of photons decreases in small fields, due to the absorption of low-energy photons inside the collimators, beam hardening occurs. Through inelastic scattering of neutrons with the internal wall of the collimator, more photons are produced and these cause the increase of neutron equivalent dose for smaller field sizes. Also as mentioned before, the comparison of neutron parameters is done for nominally same field sizes, and it should be noted that the area of these field sizes is not same and secondary collimator creates bigger field size compared to the corresponding cone field. Therefore, these reasons lead to larger equivalent dose with the secondary collimators than circular fields.

Figure 6 shows the neutron absorbed doses for different field sizes along the central axis. As it is indicated, neutron absorbed dose similar to neutron equivalent dose reaches its maximum value at the surface of the phantom and then decreases monotonically by increasing depth. Similar to equivalent dose and neutron fluence, absorbed dose in secondary collimator is more than those of circular cones. Table 5 compares neutron absorbed dose quantitatively for different field sizes. Therefore, similar to neutron equivalent dose, the photoneutron interactions increase in smaller fields and consequently the neutron absorbed dose increases in smaller fields.

As it is shown in Tables 3, 4, and 5, all neutron parameters are bigger at central axis of beam created by secondary collimator than those of circular cones. In secondary collimator and circular cone fields, photoneutron production per Gy of photon dose increases by decreasing field size. It seems that circular cones reduce the amount of neutron in central axis.

## Discussion

Secondary cancer probability is the most concerning matter in radiotherapy. One of the most important factors in increasing the secondary cancer probability is neutron contamination in megavoltage photon fields which causes extra and un-estimated dose to the patients. Therefore, it is crucial to have quantified information of neutron contamination in different treatment modalities.<sup>16</sup> In the studied treatment methods, generated neutrons in photoneutron interactions have the highest amount and energy at the surface of phantom. Therefore, at the surface of the phantom, fast neutrons will be changed to thermal neutrons, the number of neutrons will increase, and the fluence will be increased and reach a peak at specific depth (2 cm) in which all fast neutrons have been thermalised and then the number of neutrons decreases. Equivalent neutron dose and absorbed dose decrease monotonically by increasing depth in phantom. Neutron equivalent dose is related to neutron radiation quality factor which is significant for high-energy neutrons. Therefore, at the surface of the phantom, neutron equivalent dose is maximum, and by decreasing energy in depths, neutron dose will decrease linearly. Neutron absorbed



**Table 5.** Comparison of neutron absorbed doses for different field sizes<sup>7</sup>

Field size		Neutron absorbed dose ( $\mu\text{Gy}/\text{Gy}$ )	
Secondary collimator ( $\text{cm}^2$ )	Circular cone diameter (cm)	Secondary collimator jaws	Circular cones <sup>7</sup>
1 × 1	1	903	99.71
2 × 2	2	253	81.46
3 × 3	3	131	78.2

dose is directly related to neutron energies; therefore as the depth increases, absorbed dose of neutron decreases.<sup>17,18</sup> Therefore, it can be concluded that superficial organs are more affected by photoneutrons.

As the field size decreases, due to the absorption of low-energy photons in thickness of collimators, the most high-energy photons will exist in smaller fields, and by their interaction with high Z materials, the photoneutron production in smaller field will be increased. Also, since the amount of high Z materials present in the path of high-energy photons increases in smaller field sizes, the photoneutron interaction increases. Therefore, neutron fluence, neutron absorbed dose, and neutron equivalent dose increase when the field size—created either by cone or secondary collimator—gets smaller.<sup>7,19</sup>

Neutron contamination in small fields of circular cones has been reduced at the central axis in comparison to those created by secondary collimators. The reason for this phenomenon might be that: a) some of these neutrons are scattered out of the primary beam and central axis, b) neutron energy reduced which caused softer neutron spectrum, and c) although photoneutrons can be produced in circular cones, but the number of high-energy photons which can interact with circular cones are lesser compared to interacting with target and flattening filter.<sup>19,20</sup> Therefore, it seems that using circular cones in small fields can reduce the neutron contamination at central axis.

## Conclusion

The results of this study revealed delivering small photon fields by circular cones produces less neutron contamination compared to those shaped by secondary collimator jaws. Comparison of various parameters of neutron contamination in different field sizes shows that by decreasing the field size neutron fluence, neutron equivalent dose and neutron absorbed dose per Gy of photon dose in treatment field increase, and it is due to the high amount of photoneutron interactions in small fields. Additionally, organs at the surface are more influenced by neutrons, which should be considered in treatment. On the other hand, photoneutron production in the central axis of high megavoltage photon beam will decrease in the presence of circular cones.

**Competing interests.** The authors declare none.

## References

- Hosseinzadeh E, Banaee N, Nedaie HA. Cancer and Treatment Modalities. *Curr Cancer Ther Rev* 2017; 13: 1–12.
- Talebi AS, Hejazi P, Jadidi M, Ghorbani RA. Monte Carlo study on Photoneutron Spectrum around Elekta SL75/25 18 MV linear accelerator. *Int J Adv Biol Biomed Res* 2016; 4: 48–57.
- Rajesh KR, Ganapathi Raman R, Musthafa MM, Midhun CV, Joseph N. A passive method for absolute dose evaluation of photoneutrons in radiotherapy. *Int J Radiat Res* 2020; 18: 173–178.
- Naseri A, Mesbahi A. A review on photoneutrons characteristics in radiation therapy with high-energy photon beams. *Rep Pract Oncol Radiother* 2010; 15: 138–144.
- Parwaie W, Refahi S, Afkhami Ardekani M, Farhood B. Different Dosimeters/Detectors Used in Small-Field Dosimetry: Pros and Cons. *J Med Signals Sens* 2018; 8: 195–203.
- Dosimetry of small static fields used in external photon beam radiotherapy: Summary of TRS-483, the IAEA–AAPM international Code of Practice for reference and relative dose determination. *Med Phys* 2018; 45: 1123–1145.
- Hosseinzadeh E, Banaee N, Nedaie HA. Monte Carlo calculation of photoneutron dose produced by circular cones at 18 MV photon beams. *Rep Pract Oncol Radiother* 2018; 23: 39–46.
- Samiei F, Nedaie HA, Darestani H, Banaee N, Shagholi N, Mohammadi K, Shahvar A. The measurement of photoneutron dose around an 18 MV Varian linear accelerator by TLD600 and TLD700 dosimeters inside the polyethylene sphere of neutron probe LB 6411. *Adv Phys* 2014; 6: 1049–1057.
- Saeed MK, Moustafa O, Yasin OA, Tuniz C, Habbani FI. Doses to patients from photoneutrons emitted in a medical linear accelerator. *Radiati Prot Dosimetry* 2009; 133: 130–135.
- Guoqing Zh. IAEA Germany, Monte Carlo simulation of mixed neutron-gamma radiation fields and dosimetry devices. Dec 2011; 150 p; Diss. (Dr.-Ing.) (2011).
- Allahverdi M, Zabihzadeh M, Ay MA, Mahdavi SR, Shahriari M, Mesbahi A, Alijanzadeh H. Monte Carlo estimation of electron contamination in a 18 MV clinical photon beam. *Iran J Radiat Res* 2011; 9: 15–28.
- Fielding A. Monte-Carlo techniques for radiotherapy applications I: Introduction and overview of the different Monte-Carlo codes. *J Radiother Pract* 2023; 22: E80.
- Haghighat A, Wanger JC. Monte Carlo variance reduction with deterministic importance function. *Prog Nucl Energy* 2003; 42: 25–53.
- Martínez-Ovalle SA, Barquero R, Gómez-Ros JM, Lallena AM. Neutron dose equivalent and neutron spectra in tissue for clinical linacs operating at 15, 18 and 20 MV. *Radiat Prot Dosimetry* 2011; 147: 498–511.
- Ghorbani M, Vejdani Noghreiyani A, Tabatabaei ZS, Pakravan D, Davenport D. Tissue composition effect on dose distribution in radiotherapy with a 6 MV photon beam of a medical linac. *J Cancer Res Ther* 2019; 15: 237–244.
- Bahreyni Toossi MT, Khajetash B, Ghorbani M. Assessment of Neutron Contamination Originating from the Presence of Wedge and Block in Photon Beam Radiotherapy. *J Biomed Phys Eng* 2018; 8: 3–12.
- Kry S F, Howell R M, Salehpour M, Followill D S. Neutron spectra and dose equivalents calculated in tissue for high-energy radiation therapy. *Med Phys* 2009; 36: 1244–50.
- Zanini A, Durisi E, Fasolo F, Ongaro C, Visca L, Nastasi U, Burn KW, Scielzo G, Adler JO, Annand JR, Rosner G. Monte Carlo simulation of the photoneutron field in LINAC radiotherapy treatments with different collimation systems. *Phys Med Biol* 2004; 49: 571–582.
- Tajiki S, Nedaie HA, Rahmani F. A Monte Carlo study of neutron contamination in presence of circular cones during stereotactic radiotherapy with 18MV photon beams. *Biomed Phys Eng Express* 2020; 6: 1–33.
- Rezaian A, Nedaie HA, Banaee N. Measurement of neutron dose in the compensator IMRT treatment. *Appl Radiat Isot* 2017; 128: 136–141.